Mechanical Characterization of the Crystallizing Mechanism of Syndiotactic Polystyrene

Koh-hei Nitta,*,† Hisayuki Nakatani,† Hirofumi Yamada,†,‡ Masayuki Yamaguchi,§ and Kazuo Soga||

Center for New Materials and School of Materials Science, Japan Advanced Institute of Science and Technology, 1-1 Asahidai, Tatsunokuchi, Ishikawa, 923-12 Japan

Received July 31, 1997; Revised Manuscript Received January 30, 1998

ABSTRACT: A glassy film of syndiotactic polystyrene (SPS) prepared by quenching the melt into ice−water shows a recovery of the dynamic tensile moduli above glass transition temperature. The recovery process of the dynamic moduli is associated with the crystallization−nucleation process. It is found that the SPS film isothermally heated at a temperature in the recovery process shows power law relaxation behavior or a critical state like a gelation point. Furthermore, the polarized infrared and light scattering studies support that the critical state forming a three-dimensional network junctions, which act as precursors of the crystal nuclei during strain-induced crystallization, appear during the induction of crystallization.

Introduction

The synthesis of stereoregular polystyrene has been developed to produce nearly 100% syndiotactic polymer using a specific metallocene catalyst.[1−3] It has shown that syndiotactic polystyrene (SPS) is crystallizable in two different chain conformations.[4−10] SPS samples crystallized from the melt exhibit an extended all-trans planner zigzag conformation (α form) with a fiber period of 0.51 nm, showing a melting temperature of about 540 K, whereas those cast from a dilute solution form a 2-hold helical structure. The helical conformation has been shown to irreversibly transform to the α form on drawing or on heating to near 460 K, suggesting that the α form is more stable than the helical form.

As is well-known, moreover, SPS samples form a glassy state when they are quenched from the melt in ice−water.[10,11] It has been shown that the glassy SPS samples can be easily crystallized on annealing or drawing.[12] Very little is known, however, regarding molecular mechanism responsible for crystallization or nucleation proceeds from the disordered amorphous state in a quenched SPS. The present paper reports rheological and rheo-optical studies of thermal- and/or strain-induced process in glassy SPS films, with the aim of clarifying the phenomena leading to the crystallization of amorphous samples.

Experimental Section

Samples. Styrene monomer used in this study was a commercial grade supplied from Nacalai Tesque Co. The styrene was washed with an aqueous solution of sodium hydroxide, dried over calcium hydride for 24 h, and distilled under reduced pressure before use. Toluene used as solvent was purified by refuluxing over calcium hydride for 24h, followed by fractional distillation. $AlMe_3$ (TMA) and $CuSO_4 \cdot 5H_2O$ were commercially obtained and used without further purification. Methylaluminoxane (MAO) was prepared from TMA and $CuSO_4 \cdot 5H_2O$ according to the literature[13] and reserved as stock solution in toluene, 1.04 mmol/mL. η-$C_5(CH_3)_5TiCl_3$ was synthesized according to the literature.[14]

The polymerization of styrene was carried out at 303 K in a 100 mL glass reactor equipped with a magnetic stirrer under nitrogen atmosphere using toluene as the solvent. Polymerization was quenched by adding acidic methanol, and the product was filtered and dried under reduced pressure at 333 K. The polymers were then fractionated by exhaustive extraction with boiling methyl ethyl ketone in a Soxhlet extractor. Further, to separate the catalyst, the resulting samples were dissolved in xylene to make a 1% solution at 403 K and successively filtered. The filtrate was reprecipitated in a 15-fold excess of methanol to which was added a slight amount of an antioxidant, and the powder samples thus obtained were dried in a vacuum oven at 393 K for 40 h.

The microstructure of the polymer was examined by ^{13}C NMR. The 75.5 MHz ^{13}C NMR spectrum was recorded on a Varian Gemini 300 spectrometer at 403 K in C_6D_6. The [rrrr] pentad was estimated to be more than 99% from the phenyl C1 peak area.

The molecular weight and molecular mass distribution of the polymers were measured at 403 K by gel permeation chromatography (GPC) with a Senshu Scientific SSC-7100 system using *o*-dichlorobenzene as the solvent. The number average molecular weight ($\bar{M}_n$) and polydisperisity ($\bar{M}_w/\bar{M}_n$) of the SPS were 3.0×10^5 and 2.3, respectively.

To obtain amorphous films, the SPS was melted at 568 K under a press of 10 MPa and immediately quenched in ice−water. The resulting films were amorphous, as confirmed by wide-angle X-ray diffraction (see Figure 1). For comparison, slowly cooled films of the SPS were prepared by cooling (at about −2 K/min) to room temperature in press. It was confirmed from the X-ray diffraction patterns that the slowly cooled films showed the α-form crystal as shown in Figure 1.

Densities of all the films were determined by flotation in concentrated KBr solution at 303 K vis appropriate dilution.

Measurements. Measurements on the dynamic tensile moduli as well as the stress−strain behavior were made using a dynamic analyzer (Rheology Co. Ltd DVE-V4). Temperature dependences of the storage modulus E', the loss modulus E'', and the loss tangent tan δ were measured between 123 and 543 K at a heating rate of 2 K/min and at 50 Hz. To find a critical point in the transformation from the disordered state to the crystalline state, we measured tan δ at 393 K in the frequency scans between 40 and 200 Hz.

* To whom correspondence should be addressed.
† Center for New Materials.
‡ Current address: Kitami Institute of Technology, Kitami, Hokkaido, 090 Japan.
§ Current address: Yokkaichi Lab. TOSOH Corp., Yokkaichi, Mie, 510 Japan.
|| School of Materials Science.

S0024-9297(97)01157-1 CCC: $15.00
Published on Web 04/28/1998

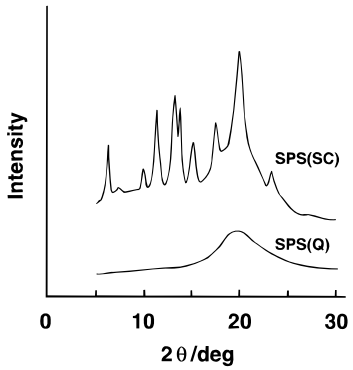

Figure 1. X-ray diffractgrams of quenched and slow-cooled SPS films.

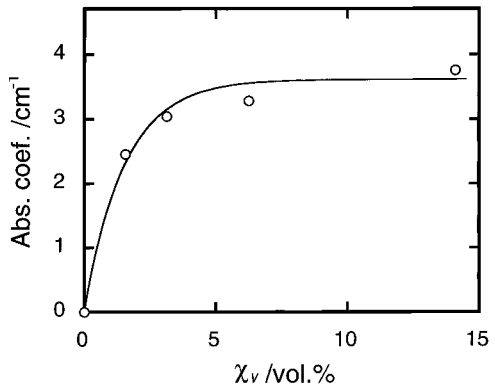

Figure 2. Variation of absorption coefficient for the 1223 cm^{-1} band with the crystallinity in volume fraction.

Infrared spectra were taken by using a JASCO FT-IR500 spectrometer. Temperature scans of infrared spectra were also made with 4 cm^{-1} resolution, with five accumulation cycles, and at a heating rate of 2 K/min using a heat-cell CHINO BD1000. The polarized infrared spectra around 1223 cm^{-1} of uniaxially oriented films were also examined with a wire-grid polarizer (JASCO PL-18).

Small-angle light scattering was performed with a commercial light scattering photometer (IST Planing SALS-100S) using the He−Ne laser (632.8 nm). The detector used was a photomultiplier that can rotate horizontally around a specimen to scan scattering angles from 0 to 20°.

Sample Characterization. The degree of crystallinity χ_v in volume fraction was determined from the density using the relation

$$\chi_v = \frac{\rho - \rho_a}{\rho_c - \rho_a} \tag{1}$$

where ρ, ρ_c, and ρ_a represent the densities of the film specimen, the crystalline part, and the amorphous part, respectively. The crystalline density ρ_c was taken to be 1033 kg/m^3 according to Greis et al.[12] and we find the amorphous density ρ_a = 1097 (±1) kg/m^3, which was measured for quenched SPS films. It is interesting to note that the amorphous density is greater than the crystalline density.

The intensity of the 1223 cm^{-1} band is completely absent in a quenched SPS film and is present only on annealing or drawing. The band has been shown to be ascribed to the methine CH deformation, which is sensitive to a sequence of trans conformation and has strong parallel polarization.[8,15] In Figure 2, the relation between the crystallinity χ_v and the absorption coefficient α for the 1223 cm^{-1} band is plotted. A crystallization kinetics analysis provides us with the following empirical relationship:

$$\alpha = 3.76(1 - e^{-0.45\chi_v}) \tag{2}$$

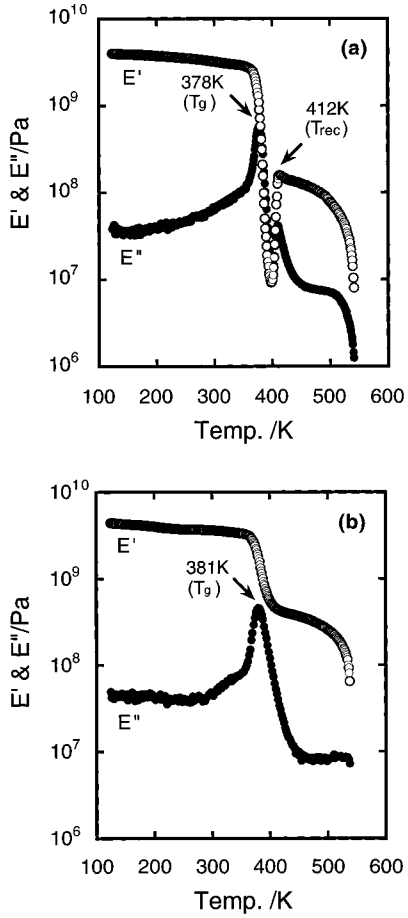

Figure 3. Temperature dependence of the storage modulus E' and the loss modulus E'' for (a) a quenched SPS film and (b) a slow-cooled SPS film.

It was found that the crystallinity of the slowly cooled SPS film was about 14%.

Results and Discussion

The temperature dependences of E' and E'' for both the quenched and slowly cooled SPS films are shown in parts a and b of Figure 3. There is a sharp peak around 380 K ascribed to glass transition T_g for both films. The loss modulus E'' of the quenched SPS film recovers in the temperature range between 400 and 412 K, and then the film shows a broad relaxation peak which can be also seen in the slowly cooled or crystallized SPS film. Therefore, it is likely that the relaxation results from the motion of chain units located within the crystalline portion of the SPS film, corresponding to the α-relaxation process as seen in semicrystalline polymers.[16] The frequency dependence of T_g in the quenched SPS gave an activation energy of 440 kJ/mol, which is comparable with that of atactic PS,[17] whereas the recovery temperature T_{rec} was found to be independent of frequency.

The derivative intensities for the 1223 cm^{-1} band are plotted against the inverse of temperature in Figure 4, where the values of E'' are also plotted for comparison. Apparently, the crystallization proceeds after the recovery of E'', suggesting that the recovery of E'' is associated with an initial stage of crystallization and/or nucleation process. The formation of α-form crystals from the amorphous state is followed by monitoring tan δ as a function of the retention or annealing time t_R at a fixed temperature of 393 K between T_g and T_{rec}. These features have been identified in numerous studies on

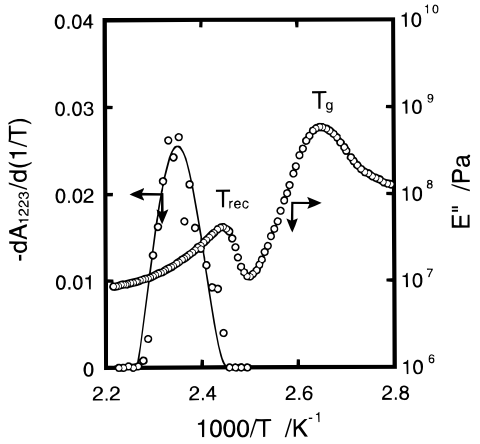

Figure 4. Variation of derivative intensity for the 1223 cm^{-1} band and loss modulus E'' with inverse of temperature for a quenched SPS film.

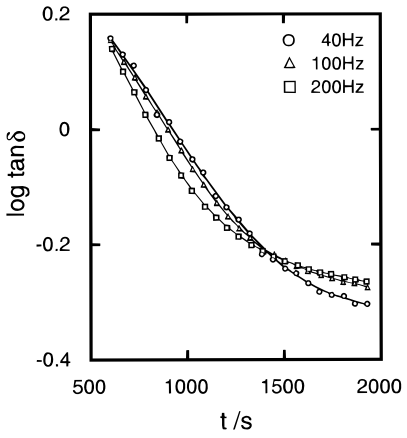

Figure 5. Variation of tan δ of a quenched SPS film with retention time at a fixed temperature of 393 K.

the gelation mechanism since the pioneering work by Winter et al.[18−22] and are shown in Figure 5. The quenched SPS film shows a critical point at $t_R = 1.4 \times 10^3$ s, in which tan δ is independent of frequency. Before 1.4×10^3 s of annealing, tan δ decreases with increasing frequency, as is typical for a viscoelastic liquid. After 1.4×10^3 s of annealing, tan δ increases with frequency, as is typical for a viscoelastic solid. At $t_R = 1.4 \times 10^3$ s, we have tan $\delta = 0.63$, which corresponds to a relaxation exponent of $n = 0.36$. It is thus suggested that the isothermal process of the SPS polymer induces the formation of a three-dimensional network structure. In this work, the power law region in the limited frequency range of 40−200 Hz failed to extend to lower and higher frequency regions because of the identification limits of our instrument.

Figure 6 shows the stress−strain curves for the SPS films annealed at 393 K for two different retention times, i.e., $t_R = 0.6 \times 10^3$ s and 2.4×10^3 s. For SPS films annealed for times shorter than 1.4×10^3 s, the stress−strain curves have a sigmoidal shape as is typical for elastomers and deviate from the Mooney−Rivlin relation,[23] as is represented as solid lines in Figure 6, beyond the elongation of around 1.5. On the other hand, it is found that the SPS films annealed for times longer than 1.4×10^3 s exhibit a yielding point as seen in semicrystalline polymeric solids.

To examine the crystallization proceeds during drawing, the absorbance components of the 1223 cm^{-1} band polarized perpendicular ($A_\perp$) and parallel ($A_\parallel$) to the fiber

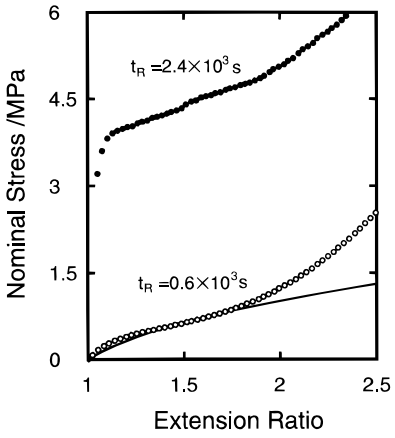

Figure 6. Stress-extension curves of SPS films isothermally heated for 2400 s and of 600 s. The solid line denotes the Mooney−Rivlin relationship.

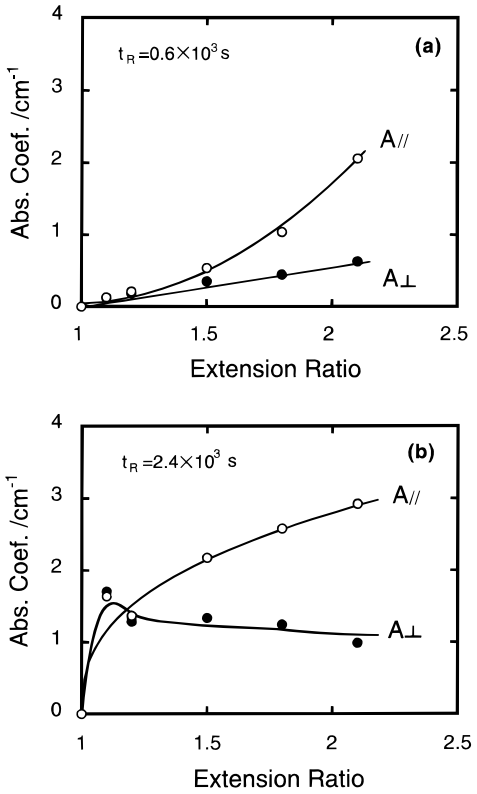

Figure 7. Absorption coefficient for the 1223 cm^{-1} band plotted against extension ratio of SPS films annealed at 393 K (a) for 600 s and (b) for 2400 s. The $A_\parallel$ and $A_\perp$ represent the absorption component the 1223 cm^{-1} band polarized parallel and perpendicular to the fiber axis, respectively.

axis were measured for the SPS films annealed at 393 K for 0.6×10^3 s and 2.4×10^3 s. Figure 7 exemplifies the absorbances of $A_\parallel$ and $A_\perp$ plotted against the extension ratio λ for the two SPS films. In the case of the SPS film annealed for 0.6×10^3 s, which is shorter than critical point (Figure 7a), the perpendicular component $A_\perp$ displays a sufficiently low value over the entire experimental strain regions and the parallel component $A_\parallel$ increases rapidly after $\lambda = 1.5$. This clearly indicates that the drawing of the SPS generates a strain-induced fibrillar crystallization[24] in the stretched direction. The high dichroism of the 1223 cm^{-1} band suggests that the crystalline trans sequence has nearly perfect orientation because the 1223 cm^{-1} band has strong parallel polarization.[8,15] Therefore, the deviation

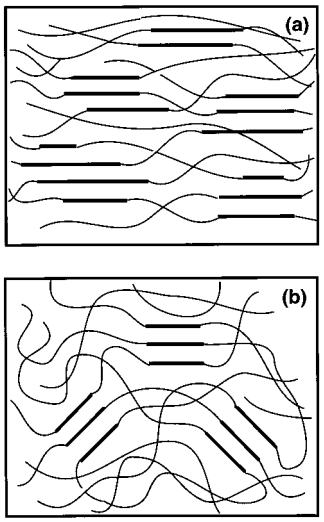

Figure 8. Schematic illustration of crystallline structure for SPS films isothermally crystallized at 393 K (a) before the critical point and (b) after the critical point.

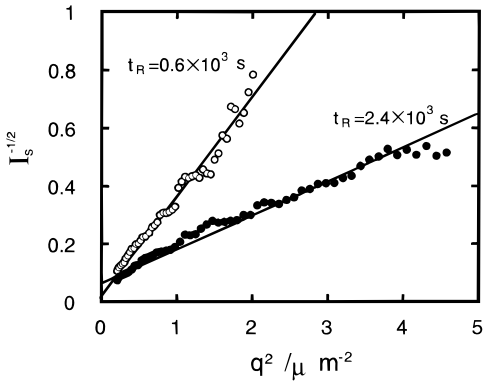

Figure 9. Debye−Bueche plots of SPS films annealed at 393 K for 600 and 2400 s.

of the stress−strain behavior from the Mooney−Rivlin equation will be responsible for the strain-induced crystallites which act to increase the modulus by forming additional physical cross-links. On the other hand, the SPS films annealed for times longer than critical point (Figure 7b) show immediate increases of the parallel component $A_{\parallel}$ and the perpendicular component $A_{\perp}$. It should be noted that the magnitude of $A_{\perp}$ remains constant over the entire experimental elongational range, suggesting a certain number of randomly oriented crystallites.[25] The immediate initiation of crystallization will be responsible for a yield point in the stress−strain curves as is typical for semicrystalline polymers. The difference in the crystallization process between the two samples is schematically shown in Figure 8.

We also investigated the crystallization processes of these samples when annealed at 393 K in the pre- and post-critical points using the small-angle light scattering (SALS) technique. As shown in Figure 9, the Debye−Bueche model[26,27] is applicable so that the correlation lengths can be derived from the ratio of slope to intercept. The correlation lengths,[28] which correspond to the distance between neighboring crystallites or crystal nuclei, are plotted against the extension ratio λ in Figure 10. The SPS film annealed for 0.6 × 10^3 s below the critical point shows a monotonic decrease with respect to λ, suggesting that the crystallites or crystal nuclei develop everywhere in the film during stretching.

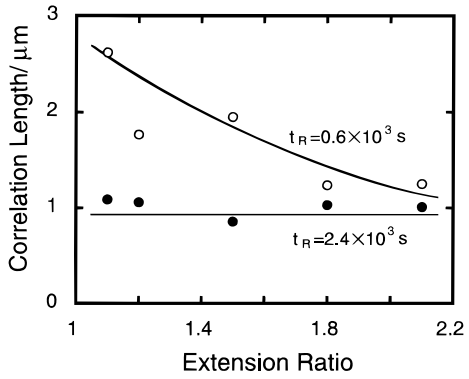

Figure 10. Correlation length of SPS films annealed at 393 K for 600 and 2400 s plotted against extension ratio.

On the other hand, for the SPS film annealed for 2.4 × 10^3 s above the critical point, the correlation length remains constant during elongation, suggesting a certain number of crystallites or crystal nuclei. The result can be understood in terms of the assumption that the crystallites or crystal nuclei develop around so-called "precursors"[29,30] forming in the critical state and the precursor behaves as three-dimensional network junctions such as a gelation point identified by the frequency-independent point of tan δ.

Conclusions

In the present paper, we have studied the crystallization mechanism of syndiotactic polystyrene (SPS) using dynamic mechanical and rheo-optical techniques. Glassy films of syndiotactic polystyrene (SPS) were prepared by quenching the melt into ice−water. The isothermal crystallization process of the glassy SPS film was investigated by monitoring the dynamic loss tangent tan δ at a crystallization temperature above the glass transition temperature. It was found that the SPS film isothermally heated during the induction period of crystallization shows power law relaxation behavior or a critical point at which tan δ is independent of frequency. To confirm the appearance of the critical state, the polarized infrared spectra and light scattering were measured during the strain-induced crystallization for SPS films annealed in the pre- and post-critical point. The results thus obtained suggested that three-dimensional network junctions, which act as a precursor of the crystal nuclei during strain-induced crystallization, are formed at the critical state.

References and Notes

(1) Ishihara, N.; Semiya, T.; Kuramoto, M.; Uoi, M. *Macromolecules* **1986**, *19*, 2464.
(2) Ishihara, N.; Kuramoto, M.; Uoi, M. *Macromolecules* **1986**, *21*, 3356.
(3) Zambelli, A.; Longo, P.; Pellecchia, C.; Grassi, A.*Macromolecules* **1987**, *20*, 2035.
(4) Tadokoro, H.; Kobayashi, M.; Kobayashi, S.; Yesufuku, K.; Mori, K. *Rep. Prog. Polym. Phys. Jpn.* **1966**, *9*, 181.
(5) Immirzi, A.; de Candia, F.; Iannelli, P.; Zanbelli, A.; Vittoria, V. *Makromol. Chem. Rapid Commun.* **1988**, *9*, 761.
(6) Vittoria, V.; de Candia, F.; Zannelli, P.; Immirzi, A. *Makromol. Chem. Rapid Commun.* **1988**, *9*, 765.
(7) Kobayashi, M.; Nakaoki, T.; Uoi, M. *Rep. Prog. Polym. Phys. Jpn.* **1988**, *31*, 481.
(8) Kobayashi, M.; Nakaoki, T.; Ishihara, N. *Macromolecules* **1989**, *22*, 4377.
(9) Guerra, G.; Vitagliaro, V. M.; de Rosa, C.; Petraccone, V.; Corradini, P. *Macromolecules* **1990**, *23*, 1539.
(10) Gomez, M. A.; Tonelli, A. E.; *Macromolecules* **1991**, *24*, 3533.

(11) Kobayashi, M.; Nakaoki, T.; Ishihara, N. *Macromolecules* **1990**, *23*, 78.
(12) Greis, O.; Xu, Y.; Asano, T.; Petermann, J. *Polymer* **1989**, *590*, 30.
(13) Sinn, H.; Kaminsky, W.; Vollmer, H. J.; Woldt, R. *Angew, Chem., Int. Ed. Engl.* **1980**, *19*, 390.
(14) Yamamoto, H.; Yasuda, H.; Tasumi, K.; Lee, K.; Nakamura, A. *Organometallics* **1995**, *8*, 105.
(15) Reynolds, N. M.; Savage, J. D.; Hsu, S. L. *Macromolecules* **1989**, *22*, 2867.
(16) Mandelkern, L. In *Physical Properties of Polymers*, 2nd ed.; American Chemical Society: Washington, DC, 1993.
(17) Tsagaropoulos, G.; Eisenberg, A. *Macromolecules* **1995**, *28*, 6067.
(18) Winter, H. H.; Chambon, F. *J. Rheol.* **1987**, *30*, 367.
(19) Hess, W.; Vilgis, T. A.; Winter, H. H. *Macromolecules* **1988**, *21*, 2536.
(20) Te Nijenhuis, K.; Winter, H. H. *Macromolecules* **1989**, *22*, 411.
(21) Scanlan, J. C.; Winter, H. H. *Macromolecules* **1991**, *24*, 47.
(22) Lin, Y. G.; Mallin, D. T.; Chien, J. C. W.; Winter, H. H. *Macromolecules* **1991**, *24*, 850.
(23) Mooney, M. *J. Appl. Phys.* **1940**, *11*, 582.
(24) Smith, K. J. *J. Polym. Sci., Polym. Phys. Ed.* **1983**, *21*, 55.
(25) Stein, R. S.; Wilson, R. P. *J. Appl. Phys.* **1962**, *33*, 1914.
(26) Debye, P.; Bueche, A. M. *J. Appl. Phys.* **1949**, *20*, 518.
(27) Debye, P.; Anderson, H. R.; Brunberger, H. *J. Appl. Phys.* **1957**, *28*, 679.
(28) Stein, R. S.; Stidhan, S. N. *J. Appl. Phys.* **1964**, *35*, 42.
(29) Imai, M.; Mori, K.; Mizukami, T.; Kaji, T.; Kanaya, T. *Polymer* **1992**, *33*, 4451.
(30) Imai, M.; Mori, K.; Mizukami, T.; Kaji, T.; Kanaya, T. *Polymer*, **1992**, *33*, 4457.

MA971157N